

# MPPT Operation for PV Grid-connected System using RBFNN and Fuzzy Classification

A. Chaouachi, R.M. Kamel, and K. Nagasaka

**Abstract**—This paper presents a novel methodology for Maximum Power Point Tracking (MPPT) of a grid-connected 20 kW Photovoltaic (PV) system using neuro-fuzzy network. The proposed method predicts the reference PV voltage guarantying optimal power transfer between the PV generator and the main utility grid. The neuro-fuzzy network is composed of a fuzzy rule-based classifier and three Radial Basis Function Neural Networks (RBFNN). Inputs of the network (irradiance and temperature) are classified before they are fed into the appropriated RBFNN for either training or estimation process while the output is the reference voltage. The main advantage of the proposed methodology, comparing to a conventional single neural network-based approach, is the distinct generalization ability regarding to the nonlinear and dynamic behavior of a PV generator. In fact, the neuro-fuzzy network is a neural network based multi-model machine learning that defines a set of local models emulating the complex and non-linear behavior of a PV generator under a wide range of operating conditions. Simulation results under several rapid irradiance variations proved that the proposed MPPT method fulfilled the highest efficiency comparing to a conventional single neural network.

**Keywords**—MPPT, Neuro-Fuzzy, RBFN, Grid-connected, Photovoltaic

## Nomenclature

Symbol	Quantity	Symbol	Quantity
$e$	Electron charge, $e=1.602 \cdot 10^{-19}$	$N_M$	Modules in series in an array
$I_d$	Diode current [A]	$N_P$	Parallel branches in a module
$I_0$	Reverse saturation current [V]	$N_S$	Cells in series in a module
$I_{sc}$	Short-circuit current [A]	$P_{max}^M$	Power under standard conditions
$I_{sc}^M$	Short-circuit current under standard conditions	$V_d$	Diode voltage [A]
$G_a$	Irradiance	$V_{oc}^M$	Open voltage under standard conditions
$K$	Boltzmann constant, $k=1.381 \cdot 10^{-23}$ [J/K]	$T_c$	Cell temperature [°C]
$N_B$	Parallel branches in an array	$\eta$	Diode ideality factor

**A. Chaouachi**, Department of Electronic and Information Engineering, Tokyo University of Agriculture and Technology, 2-24-16, Nakamachi, Koganei-shi, Tokyo 184-8588, Japan (e-mail: A.chaouachi@gmail.com, Tel & FAX: +81-42-388-7481)

**R.M. Kamel**, Department of Electronic and Information Engineering, Tokyo University of Agriculture and Technology, 2-24-16, Nakamachi, Koganei-shi, Tokyo 184-8588, Japan (r\_m\_kamel@yahoo.com).

**K. Nagasaka** Department of Electronic and Information Engineering, Tokyo University of Agriculture and Technology, 2-24-16, Nakamachi, Koganei-shi, Tokyo 184-8588, Japan (bahman@cc.tuat.ac.jp).

## I. INTRODUCTION

THE Kyoto agreement on global reduction of greenhouse gas emission has prompted interest on renewable energy systems worldwide. Nowadays photovoltaic energy is one of the most popular renewable sources since it is clean, inexhaustible and requires little maintenance. However, it still presents a lake of competition comparing to conventional energy resources due to its high cost and low efficiency during energy conversion. Regarding to this, it is necessary to optimize the performance of PV systems through the operation of conversion systems to increase the output efficiency of the overall system. This approach is commonly named as MPPT, several methods are referred in the bibliography: the P&O method is the most commonly used in practice due to its simplicity and ease of implementation, however, this algorithm can fail or oscillate around the Maximum Power Point (MPP) under sudden sunlight changes [1, 2]. Incremental conductance is also commonly used as it can overcome some aspects of the P&O algorithm instabilities, nevertheless this method involves current and voltage differentiation which requires a relatively complex decision making process and therefore needs more complex calculation capacity and memory [3]. More recently Artificial Neural Network (ANN) techniques are being employed for photovoltaic applications, mainly because of their symbolic reasoning, flexibility and explanation capabilities that are useful to deal with strong nonlinearities and complex systems [4]. Theodore et al proposed a MPPT for solar vehicle based on ANN reference voltage estimation [5]. Bahgat et al proposed a neural network based MPPT for a PV module supplying a dc motor that drives an air fan [6]. Preliminary results shows high MPPT efficiency for such methods [1]. On the other hand, neural networks are still considered as unstable learning model regarding to the presence of noisy sets, large training set, underfitting and overfitting problems that causes a lack of generalization and trapping on local minima solutions [7-8]. Moreover, due to the high nonlinearity and close dependence on weather conditions of PV generators, a neural network based model requires the use of a rich training set covering a wide range of climatic conditions that leads to delicate generalization ability.

This paper presents a new MPPT methodology based on a more robust estimator consisting of multi-model machine learning. The multi-model approach supposes the definition of a set of three models by means of fuzzy classification, each model consists of a Radial Basis Functions Neural Network

(RBFNN) that emulates the behavior of the PV generator for a specific climatic conditions, so-called “class”. The proposed classifier consists of transparent rules-based fuzzy classifier, such rules, unlike opaque or uninterruptable classification are straight forwarded and simple to understand. The multi-model approach aims to decrease the process complexity of the system under wide operating conditions frame, therefore the proposed estimator offers a distinct improvement regarding to the generalization capability comparing to a single ANN estimator.

## II. OVERVIEW OF THE SIMULATION SYSTEM

Fig. 1 shows the overall of the studied system, composed of a 20 kW photovoltaic generator connected to the main electric grid via two power electronics stages. The first stage consists of a DC-DC converter that insures impedance adaptation between the generator and the load by tracking the reference voltage estimated by the neuro-fuzzy network. While the second stage is composed of a DC bus and a PQ inverter that injects the power generated by the PV generator into the main grid, where the inverter is acting as power controller ensuring a high power factor. In the following subsections, all the components of the grid connected PV system are described in details.

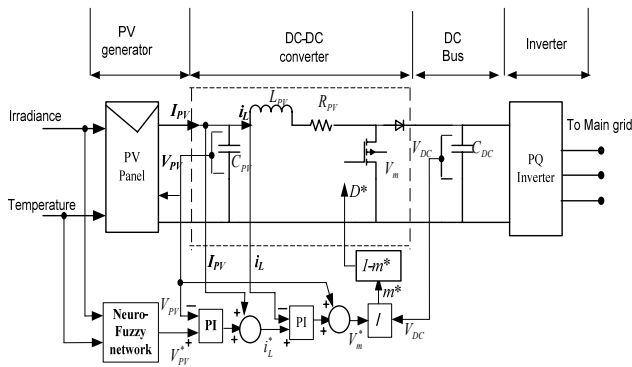


Fig. 1: Overview of the neuro-fuzzy MPPT grid connected photovoltaic system

### A. Photovoltaic system

The studied grid-connected PV system comprises a 20 kW photovoltaic generator installed at the Engineering Campus of the Tokyo University of Agriculture and Technology. A dynamic simulation model of the photovoltaic system is designed under Matlab Simulink® environment to analyze the behavior and the performances of the proposed MPPT algorithm.

A simple equivalent circuit for a PV cell consists of a real diode associated to a parallel ideal current source delivering a proportional current to the solar irradiance, from where the following relations can be expressed [9]:

$$I = I_{sc} - I_d \quad (1)$$



Fig. 2: The studied photovoltaic field installed in Tokyo University of Agriculture and Technology

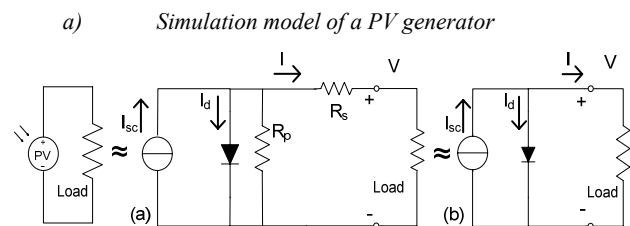


Fig. 3: (a) Equivalent circuit with added  $R_s$  parallel and  $R_p$  serial resistance (b) Photovoltaic generator equivalent simple circuit

$$\text{Where} \quad I_d = I_0 (e^{eV_d/\eta K T_c} - 1) \quad (2)$$

$$\text{Therefore} \quad I = I_{sc} - I_0 (e^{eV_d/\eta K T_c} - 1) \quad (3)$$

To deal with the dynamic behavior of a PV generator, some parallel leakage resistance  $R_p$  and a series resistance  $R_s$  (associated to the resistance of the semiconductor) should be included (Fig. 3(a)). However, for the proposed simulation, taking into account both of series and parallel resistances results in computational limitations subjected to the implicit nonlinear nature of the simulation model. Therefore, such approach is usually avoided in the photovoltaic systems bibliography. For the proposed simulation model, the parallel resistance is neglected while the series resistance  $R_s$  is considered which represents the internal resistance and the connections between cells, the mathematical relations established afterwards describing the PV generator model is expressed as following:

$$I = I_{sc} - I_0 \left\{ \exp \left( \frac{e(V + I R_s)}{\eta K T_c} \right) - 1 \right\} \quad (4)$$

Considering the case of a photovoltaic generator module (panel), composed of  $N_p$  parallel branches, each including  $N_s$  solar cells associated in series, the current delivered by a photovoltaic module under constant weather conditions can be expressed in the equation (5):

$$I^M = I_{sc}^M \left[ 1 - \exp \left( \frac{V^M - V_{oc}^M + R_s^M I^M}{N_s V_T^c} \right) \right] \quad (5)$$

The module current has an implicit expression depending on the following variables expressed in function of single cell parameters:

Short circuit current	$I_{sc}^M = N_p I_{sc}^C$
Open circuit voltage	$V_{oc}^M = N_s V_{oc}^C$
Thermal voltage in the Semiconductor	$V_T^M = (kT/q)/N_p$
Equivalent serial resistance of the module	$R_s^M = R_s^C / N_p$

As a first step, under the assumption that all the PV cells are identical, the fundamental simulation parameters for a solar cell (in standard conditions) are expressed using the module characteristics provided by the manufacturer's catalogue (Appendix 1):

$$P_{max_o}^C = \frac{P_{max_o}^M}{N_s N_p} \quad (6)$$

$$V_{oc_o}^C = \frac{V_{oc_o}^M}{N_s} \quad (7)$$

$$I_{sc_o}^C = \frac{I_{sc_o}^M}{N_p} \quad (8)$$

Now, the instantaneous series resistance of a solar cell can be expressed as:

$$R_s^C = \left( 1 - \frac{FF}{\frac{P_{max_o}^C}{V_{oc_o}^C I_{sc_o}^C}} \right) \cdot \frac{V_{oc_o}^C}{I_{sc_o}^C} \quad (9)$$

Where FF is the Fill Factor and given by the equation (10):

$$FF = \frac{\left( \frac{V_{oc_o}^C}{V_{T_o}^C} \ln \left( \frac{V_{oc_o}^C}{V_{T_o}^C} + 0.72 \right) \right)}{\frac{V_{oc_o}^C}{V_{T_o}^C} + 1} \quad (10)$$

Operating condition parameters can be calculated for a fixed voltage  $V^M$ , temperature  $T_a$  and irradiance  $G_a$  using the cell parameters in standard conditions. The short circuit current is proportional to the irradiance and can be expressed as in equation (11):

$$I_{sc}^C = \frac{I_{sc_o}^C}{G_{a_o}} \cdot G_a \quad (11)$$

The open circuit voltage of the cell is depending on the nominal open circuit voltage and the actual weather conditions which can be expressed using the following relation:

$$V_{oc}^C = V_{oc_o}^C + 0.03 \cdot (T_a + 0.03 \cdot G_a - T_o^C) \quad (12)$$

Now, the instantaneous current debited by a photovoltaic module can be finally expressed for the fixed parameters ( $V^M, T_a, G_a$ ):

$$I^M = N_p \cdot I_{sc}^C \left[ 1 - \exp \left( \frac{V^M - N_s V_{oc}^C + I^M R_s^C \frac{N_s}{N_p}}{N_s V_T^C} \right) \right] \quad (13)$$

Considering the case of a photovoltaic array that consists in  $N_B$  parallel branches, each containing  $N_M$  modules associated in series. For a  $V^M$  applied voltage, the array current is equal to  $I = \sum_{i=1}^{N_B} I_i^M$ . If we assume that all the panels are identical and

under the same temperature and irradiance, then the total current generated by the array can be expressed as following:

$$I = N_B \cdot I^M \quad (14)$$

#### b) Influence of temperature and irradiance on PV operating

Fig. 4 shows the behavior of a photovoltaic panel simulation in accordance to temperature and irradiance variations under respectively constant irradiance and temperature. In fact, a PV generator connected to a load can operate in a large margin of current and voltage depending on weather conditions [10]. Fig. 4 shows that the open circuit voltage is increasing following a logarithmic relationship with the irradiance and decreasing slightly as the cell temperature increases. On the other hand, the short circuit current is linearly depending on the ambient irradiance in direct proportion, while the open circuit voltage decrease slightly as the cell temperature increases.

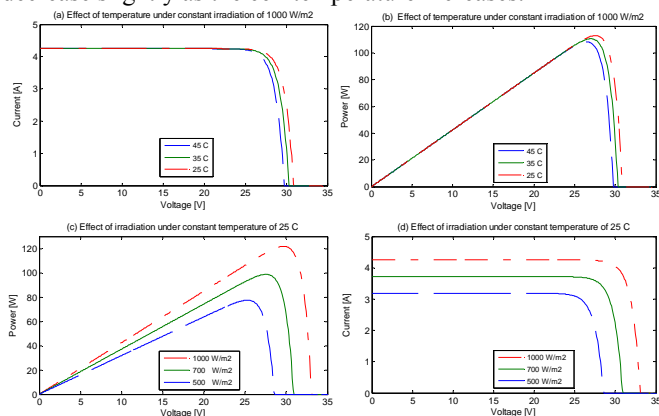


Fig. 4: Temperature (a) and irradiance (d) effects on the IV curve of a PV generator

Temperature (b) and irradiance (c) effects on the power curve of a PV generator

Therefore, the maximum power that could be generated by a PV system is slightly depending on the temperature and irradiance variations: the maximum power increases as the irradiance increases and vice versa, on the other hand a PV generator performs better for low temperature than raised one.

#### B. DC-DC boost converter

The operating point of a PV generator connected to a load is the intersection of the load curve and the PV current-voltage characteristics. In case of resistive load, the load characteristic is a straight line with slope ( $IV = 1/R$ ), while the power delivered to the load depends on the value of the resistance only. It should be pointed out that if the load R is equal to a certain optimal load  $R_{opt}$ , the PV generator delivers the Maximum Power (MP). However, if the load R is noticeably larger or smaller than  $R_{opt}$  the PV generator operates respectively as constant voltage source or constant current source.

To overcome this undesired effects on the PV power output, an electrical tracking have to be achieved through a power conditioning converter (DC-DC converter) inserted between

the load and the source to insure an impedance adaptation by matching the load impedance with the varying PV source. In other words, the DC-DC boost converter is used to maximize the energy transfer from the photovoltaic generator to an electrical system by adjusting the PV generator output voltage to a reference value ( $V_{ref}$ ) at which the PV generator supplies the maximum power.

The proposed DC-DC converter includes two power accumulation elements and thus two controllable variables which are the  $V_{pv}$  voltage and the inductor current ( $i_L$ ), a mathematical model describing the DC-DC converter can be expressed in the following relation [11]:

$$\begin{pmatrix} V_m \\ - \\ i_{ac} \end{pmatrix} = m \begin{pmatrix} V_{DC} \\ - \\ i_L \end{pmatrix} \quad (15)$$

Where  $m = 1 - D$  and  $D$  is the duty cycle of the converter switch expressed as:

$$D = \frac{t_{on}}{T} = t_{on} f_s \quad (16)$$

Where  $f_s$  is the switching frequency of the converter switch,  $t_{on}$  the time which the switch is turned on during a complete period  $T$ .

$$\frac{di_L}{dt} = \frac{1}{L_{pv}} (V_m - V_{pv}) - \frac{R_{pv}}{L_{pv}} i_L \quad (17)$$

$$\frac{dV_{pv}}{dt} = \frac{1}{C_{pv}} (i_L - i_{pv}) \quad (18)$$

The voltage control loop with the PV current compensation gives the reference current  $i_L^*$  that can be calculated using the equation (17):

$$i_L^* = PI(V_{pv}^* - V_{pv}) + i_{pv} \quad (19)$$

Where  $V_{pv}^*$  is the reference voltage calculated by the neuro-fuzzy logic controller (Fig. 1)

The optimal switching voltage is expressed using (18) and (19):

$$V_m^* = PI(V_{pv}^* - V_{pv}) + V_{pv} + \frac{R_{pv}}{L_{pv}} i_L \quad (20)$$

The controller parameters are chosen to maintain constant PV voltage and to minimize the current ripple. The DC-DC converter command is obtained by the inversion of equation (15), expressed as following in the equation (21):

$$m^* = \frac{V_m^*}{V_{DC}} \quad (21)$$

With optimal duty cycle  $D^* = 1 - m^*$

A DC link insures an energy balance between the power generated by the PV generator and the power injected into the network by charging or discharging the capacitor, that oscillate between two levels depending on the actual climatic conditions and the power injected.

### C. PQ inverter

The inverter plays a vital role in grid-connected systems, by interfacing the PV generator with the main utility power system, the configuration of a basic inverter connected to a PV generator is shown in Fig.5.

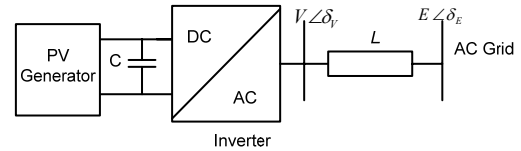


Fig. 5: Basic inverter interfaced to a grid-connected PV generator

The basic and minimum requirement of voltage source inverter is to control the flow of active and reactive power between the PV source and the main utility, the mathematical relations for P&Q magnitudes can be expressed as following in the equations (22) and (23) [12]:

$$P = \frac{VE}{\omega L} \sin(\delta_V - \delta_E) \quad (22)$$

$$Q = \frac{V^2}{\omega L} - \frac{VE}{\omega L} \cos(\delta_V - \delta_E) \quad (23)$$

As the main objective of the current work is to analyze the MPPT proposed methodology during steady state operation, it would be of no advantage to consider the details of inverter switching. Moreover, if such details are considered, then extra efforts should be done to compensate the undesired effects of the generated harmonics that leads to more heavy computational simulations. Thus, the proposed inverter is represented by its control function while the fast transients related with the commutations of the switches are not considered, therefore the power injected at the AC side does not include harmonics, losses or delays. The inverter voltage is represented using the following three controlled sinusoidal voltage sources defined as:

$$V_a = \sqrt{2} V \sin(\omega t + \delta_V) \quad (24)$$

$$V_b = \sqrt{2} V \sin\left(\omega t + \delta_V - \frac{2\pi}{3}\right) \quad (25)$$

$$V_c = \sqrt{2} V \sin\left(\omega t + \delta_V + \frac{2\pi}{3}\right) \quad (26)$$

While the control variables are  $V$  and  $\delta_V$

The basic structure of PQ inverter controller is shown in Fig.6, two PI controllers would suffice to control the flow of active and reactive powers by generating the proper values of voltage ( $V$ ) and angle ( $\delta_V$ ) based on the instantaneous value of voltage and current. The reference power ( $P_{ref}$ ) in Fig.6 represents the amount of active power produced by the photovoltaic generator interfaced to the main utility through the inverter, while  $Q_{ref}$  represents amount of reactive power desired to be injected into or absorbed from the main utility. In the present case, the inverter is operating at unity power factor ( $Q_{ref}=0$ ) therefore no reactive power is exchanged and the total

MP extracted from the PV generator is injected to the grid.

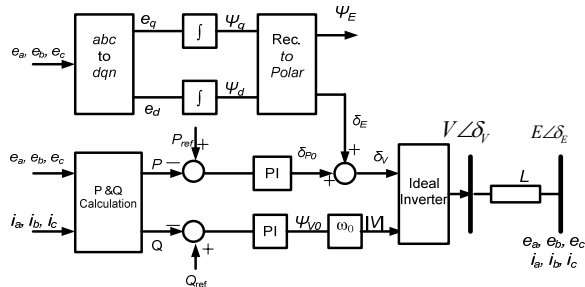


Fig. 6: Basic structure of the inverter PQ control scheme

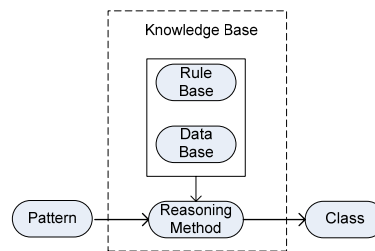


Fig. 8: Fuzzy rule-based classification system

### III. NEURO-FUZZY MAXIMUM POWER POINT ESTIMATION

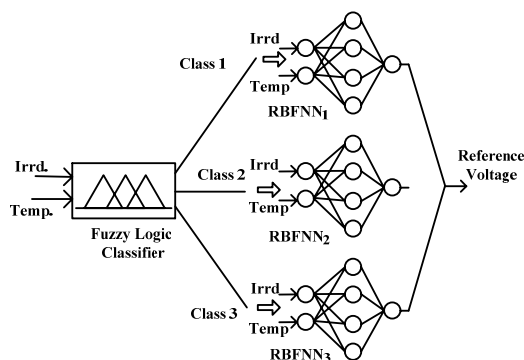


Fig.7: Architecture of the Neuro-fuzzy network

The neuro-fuzzy network consists of two stages; the first one is a fuzzy-rule based classifier while the second one is composed of three RBFNNs (Fig. 7). The three networks have similar architecture, composed of three layers: input, hidden and output layers. The main advantage of the proposed methodology comparing to a conventional single ANN estimator is the distinct generalization ability. In fact the neuro-fuzzy network is a neural network based multi-model machine learning that defines a set of local models emulating faithfully the complex and nonlinear behavior of a PV generator under a wider range of operating conditions (weather conditions).

#### A. Fuzzy rules-based classification

Classification task consists of assigning a class  $C_j$  from a predefined class set  $C = \{C_1, C_2, \dots, C_M\}$  to an object belonging to a certain feature space  $x \in S^N$ , so the problem comes to find a mapping defined as [13]:

$$D : S^N \longrightarrow C \quad (27)$$

A fuzzy rule-based classification system is composed of Fuzzy Reasoning Method (FRM) and a Knowledge Base (KB) consisting in Rule Base (RB) and data base that describes the semantic of the fuzzy subsets associated to linguistic labels on the if-then part of the rules. Basing on the KB, the FRM determine a label class for admissible patterns as shown in the Fig. 8. [14]

Let a rule base  $R = \{R_1, R_2, \dots, R_L\}$  and  $r_j$  rules in  $R$ , the RBs are generated basing on fuzzy rules with a class in the consequent according to the following structure:

$$R_k: \text{If } a_1 \text{ is } L_1^k \text{ and } \dots \dots a_N \text{ is } L_N^k \text{ then } O \text{ is } C_j \quad (28)$$

Where,

$a_1, \dots, a_N$  are the outstanding selected features for the classification task

$L_1^k, \dots, L_N^k$  are linguistic labels to discretize the continuous domain of the variables

$O$  is the class  $C_j$  to which the pattern belongs.

#### a) Fuzzy reasoning method

A fuzzy reasoning method is an inference procedure that derives conclusions from a set of if-then rules and a pattern, such methodology aims to improve the generalization capability of a classification system [13]. While each rule  $r_j$  in  $R$  generates a class  $C_j$  related to a pattern  $P^t = (p_1^t, \dots, p_N^t)$ , the FRM considers the rule with the highest combination between the matching degree of the pattern with the if-then part and the certainty degree for the classes. In fact, for each class  $C_j$ , the association degree of the pattern with the class  $O_j$  can be expressed as following:

$$O_j = \max_{k \in L} R^k(P^t) \quad (29)$$

Where,  $R^k(P^t)$  is the strength of activation (matching rule) associated to the  $k^{\text{th}}$  rule, obtained by applying a t-norm to the degree of satisfaction of the inputs patterns to the clause ( $a_1$  is  $L_1^k$ ):

$$R^k(P^t) = T(\mu_{L_1^k}^k(p_1^t), \dots, \mu_{L_N^k}^k(p_N^t)) \quad (30)$$

Finally the classification for the pattern  $E^t$  is the class  $C_h$  such:

$$O_h = \max_{j=1, \dots, M} O_j \quad (31)$$

This approach can be graphically represented by the Fig. 6:

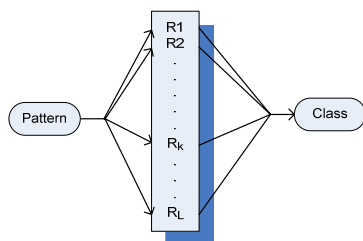


Fig. 9: Fuzzy reasoning method

#### b) Fuzzy controller Design

The fuzzy rule-based classifier was build and designed under Matlab fuzzy logic toolbox and lately exported into Simulink environment as a part of the neuro-fuzzy network and the whole simulation system.

*Membership functions:*

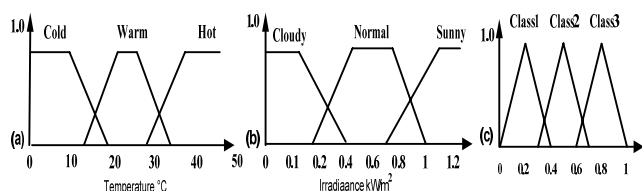


Fig. 10. Inputs and output membership functions of the fuzzy classifier

A membership function is a curve that defines how each point in the input or output space is mapped to a membership value between 0 and 1. Fig. (10a-b) shows the temperature and irradiance membership functions in trapezoidal shape, the temperature membership function is sorted into three categories labeled as: hot, worm and cold, while the irradiance membership function is sorted into three categories labeled as sunny, normal and cloudy. The output of the fuzzy system is the class associated to the inputs pattern, the Fig. (10, c) shows the output membership function in triangular shape, sorted into three categories: class1, class2 and class3.

*Fuzzy rules:*

The influence of climatic conditions on the model or behavior of a PV generator can be interpreted through linguistic conditional statements that describe the correlation between the climatic conditions and the PV operating behavior. Indeed, if-then statement based transparent rules, similar to those used in fuzzy control are established based on human expertise on the influence of weather conditions on PV systems operating characteristics that are summarized in Table. 1.

*Defuzzification:*

The fuzzy outputs for all rules are finally aggregated to one fuzzy set that need to be defuzzified so that one representative class output related to the input patterns is obtained. The centroid method (also called as “center of area” or “center of gravity”) is used for the defuzzification process. This method is the most relevant and physically appealing among the benchmark defuzzification methodology [15], the center of the

area of the combined membership functions is calculated basing on the following algebraic expression:

$$z^* = \frac{\int \mu(z).z.dz}{\int \mu(z).dz} \quad (32)$$

Where  $z$  is the defuzzified value and  $\mu$  is its associated membership function.

TABLE I FUZZY RULES ASSIGNMENT

		Irradiance		
		Cloudy	Normal	Sunny
Temperature	Cold	Class2	Class3	Class3
	Worm	Class1	Class2	Class3
	Hot	Class1	Class1	Class2

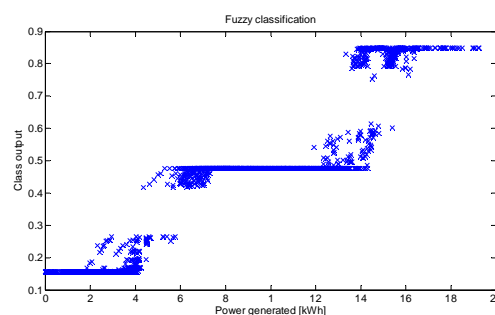


Fig. 11: Clustering of the input patterns (training data)

#### B. Radial Basis Function Neural Network

RBNN's have been successfully employed in many real world tasks in which they have proved to be a valuable alternative to MLPNN's since it requires less computing power and time. These tasks include chaotic time-series prediction, speech recognition, and data classification [16]. Furthermore, given a sufficient number of hidden units a RBNN is considered as a universal approximator for any continuous functions. [17]. The construction of a RBNN in its most basic structure (Fig. 12) involves three layers with entirely different roles. The input Layer is made up of a source node that connects the network to its external environment, the second layer which is the only hidden layer in the network, applies a non linear transformation from the input space to the hidden space. In most applications the hidden space is of high dimensionality, which is directly related to the network capacity to approximate a smooth input-output mapping. The output layer is linear, supplying the response of the network to the pattern applied to the input layer [18].

If we consider a RBNN with a single output node that computes a linear combination of the hidden units outputs, parameterized by the weights  $w$  between hidden and output layers, the function computed by the network is therefore expressed as:

$$f(\xi, w) = \sum_{b=1}^k W_b S_b \quad (33)$$



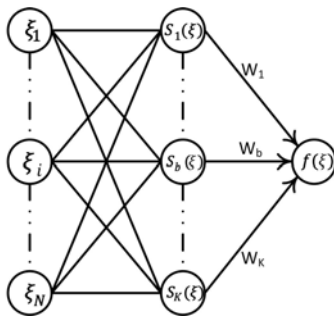


Fig. 12: Architecture graph of a RBFNN

Where  $\xi$  is the vector applied to the input units and  $S_b$  denotes the basis function  $b$ , each of the  $N$  components of the input vector  $\xi$  feeds forward to  $k$  basis functions whose outputs are linearly combined with weights  $\{W_b\}_{b=1}^k$  into the network output  $f(\xi, w)$ . The most common choice for the basis functions is the Gaussian, in this case the function computed becomes:

$$f(\xi, w) = \sum_{b=1}^k W_b \left( \frac{-\|\xi - m_b\|^2}{2\sigma_b^2} \right) \quad (34)$$

Where each hidden node is parameterized by two quantities: the center  $m$  in input space, that corresponds to the vector defined by the weights between the node and the input nodes, and the width  $\sigma_b$ .

To evaluate the performance of the proposed neuro-fuzzy network comparing to a conventional neural network based MPPT method, a single RBFNN estimator was developed besides the three ANN's (RBFNN1, RBFNN2 and RBFNN3) constituting the neuro-fuzzy learning machine. The networks inputs are temperature and irradiance while the output is the optimal reference voltage.

The training data base was recorded during the year 2008 for the training and testing process the original set was split into two subsets: training set (70%) and testing set (30%) to evaluate the generalization performance of the developed ANNs. To improve the training convergence performances, mean 0 and standard deviation 1 based across channel normalization [19] was used for the input training set rescaling, basing on the following relation:

$$S_i = \frac{x_i - \text{mean}}{\sqrt{\frac{\sum_{i=1}^N (x_i - \text{mean})^2}{N-1}}} \quad (35)$$

where  $\text{mean} = \frac{\sum_{i=1}^N x_i}{N}$

$x_i$  is the raw input variable  $X$  in the  $i^{\text{th}}$  training case

$S_i$  is the standardized value corresponding to  $x_i$

$N$  is the number of training case

The target data set was linearly normalized in order to force the network values to be within the range of output activation functions using upper ( $Y_{\max}$ ) and lower bounds ( $Y_{\min}$ ) for the values:

$$Z_i = \frac{Y_i - (Y_{\max} - Y_{\min})/2}{(Y_{\max} - Y_{\min})/2} \quad (36)$$

where  $Y_i$  is the raw target variable  $Y$  for the  $i^{\text{th}}$  training case.

$Z_i$  is the standardized value corresponding to  $Y_i$ .

RBFNN was evolved to get round over fitting problem in relation to the choice of the network framework. In fact, unlike the conventional neural networks the number of hidden nodes of a RBFNN is determined during the training and might get a big number as a couple of hundred [20]. Reducing the number of hidden neurons requested for the RBFNN training convergence is subject to several researches mainly based on optimization algorithms that allow pruning of superfluous neurons inserted for outlier, noisy and overlapping data.

#### IV. SIMULATION RESULT

Several performance criteria are reported in the ANN literature as: the training time, the modeling time and the prediction error. In the present study, as the training process is in offline mode, the first two criteria are not considered to be relevant. Thereby, the estimation performances of the neuro-fuzzy network and the single ANN will be evaluated only in term of estimation error defined as the difference between the experimental and the power efficiency.

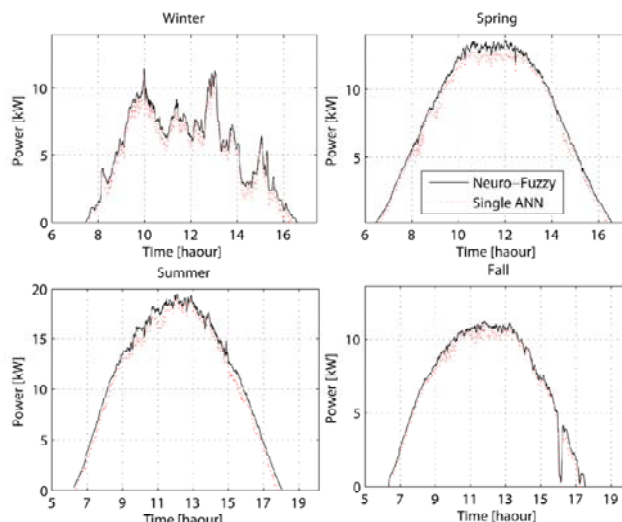


Fig. 13: Power generation comparison using Neuro-fuzzy, single ANN

To evaluate the reliability performances of the developed Neuro-fuzzy network for different ranges of climatic conditions, four days was picked up randomly from each season namely: Winter (December, January and February), Spring (March, April, May), Summer (June, July and August) and Fall (September, October and November). The Fig. 13 shows clearly that the proposed Neuro-fuzzy network fulfilled a higher MPPT efficiency comparing to the single ANN. In fact, the proposed neuro-fuzzy-based method achieved the highest power efficiency with 6.55 % of extra generated power comparing to the single RBFNN.

In order to validate the stability performances of the proposed MPPT based neuro-fuzzy estimator, we proceeded to observe the tracking of the MP during the grid connection operation. Fig. (14, a) shows the tracking of the reference voltage estimated by the neuro-fuzzy machine learning after a weather condition step change (irradiance  $650 \rightarrow 500 \text{ kW/m}^2$ ; temperature  $26.5 \rightarrow 24.5^\circ\text{C}$ ) basing on experimental measures. In fact, the neuro-fuzzy network supplies a new value of reference voltage, tracked through the DC-DC stage so that the overall system can keep operating under optimal conditions, that is to say that the power injected into the main utility is equal to the MP (Fig. (14, b)) throughout the steady-state next to the climatic disturbance. Fig. (14, c) shows the variation of the current generated by the PV array after the climatic perturbation basing on the new set point of the system optimal operation meanwhile the RMS voltage keep stable (Fig. (14, d)).

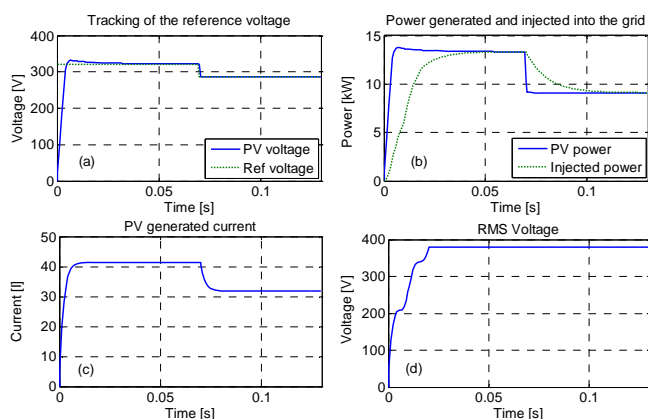


Fig. 14: Operating during a weather condition step

Fig. 15 shows the current injected into the main utility and the grid side voltage before and after the weather conditions step change. As it can be seen, the voltage and current are in phase which means that the MP extracted from the PV array can pass into the main grid as the whole system operates at unity power factor ( $Q_{\text{ref}} = 0$ ) with no reactive power exchange.

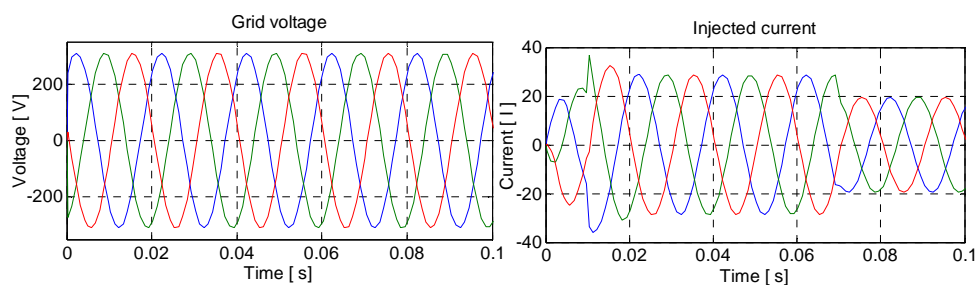


Fig. 15: Injected current and grid side voltage during a weather condition step


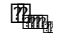
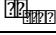


## V.CONCLUSION

In this paper a new MPPT methodology applied to a grid-connected photovoltaic system based on a neuro-fuzzy estimator is proposed and investigated. The whole system was simulated under Matlab Simulink® environment, the developed neuro-fuzzy network consists of two stages; the first one is a fuzzy rule-based classifier, the second one is composed of three multi-layered feed forwarded ANNs trained offline using experimental data from a real PV system installed at Tokyo University of Agriculture and Technology. The proposed neuro-fuzzy estimator can faithfully emulate the dynamic and nonlinear behavior of a photovoltaic generator under a large wide of climatic conditions. In fact the multi-model aspect of the proposed machine learning confer it a distinct generalization ability comparing to a conventional single ANN-based MPP predictor. Maximum power operation was achieved by tracking the reference voltage estimated by the neuro-fuzzy network through a DC-DC converter. The whole grid-connected system performance was tested during a cloudy day with several rapid irradiance variations. The simulation results showed that the proposed system performances was not degraded, as the MPPT dispositive was able to track the reference voltage insuring an optimal operating condition under any rapid changing meteoric conditions.

## APPENDIX

### PV MODULE SPECIFICATION

<b>Manufacturer</b>	SHARP	<b>Maximum power</b>	120 W
<b>Type</b>	NE-LO1A		31.9 V
<b>Maximum voltage</b>	600 V		5.31
<b>Weight</b>	12.5 Kg		25.7

## REFERENCES

- [1] D. P. Hohm and M. E. Ropp "Comparative Study of Maximum Power Point Tracking Algorithms" Progress in photovoltaics: research and applications, 2003, pp. 47-62.
- [2] V. Salas, E. Olías, A. Barrado, A. Lazaro, "Review of the maximum power point tracking algorithms for stand-alone photovoltaic systems", Solar Energy Materials & Solar Cells 90, 2006, pp. 1555-1578.
- [3] Trishan Eram, Patrick L. Chapman, "Comparison of Photovoltaic Array Maximum Power Point Tracking Techniques", IEEE Transactions On Energy Conversion, Volume. 22, Number. 2, 2007, pp. 439-449.
- [4] Adel Mellit, and Soteris A. Kalogirou "Artificial intelligence techniques for photovoltaic applications: A review", Progress in Energy and Combustion Science 34, 2008, pp. 574-632.
- [5] Theodore Amissah OCRAN, Cao Junyi, Cao Binggang, Sun Xinghua, "Artificial Neural Network Maximum Power Point Tracker for Solar Electric Vehicle" Tsinghua science and technology ISSN 1007-0214 12/23 Volume 10, Number 2, 2005, pp. 204-208.
- [6] A.B.G. Bahgat, N.H. Helwa, G.E. Ahmad, E.T. El Shenawy, "Maximum power point tracking controller for PV systems using neural networks", Renewable Energy 30, 2005, pp 1257-1268.
- [7] ZHANG Gao, FAN Ming, ZHAO Hongling, "Bagging Neural Networks for Predicting Water Consumption," Journal of Communication and Computer, Volume 2, No.3 Serial No.4, 2005, pp: 19-24.

- [8] Xavier Anguera, Takahiro Shinozaki, Chuck Wooters and Javier Hernando, "Model Complexity Selection and Cross-Validation EM Training for Robust Speaker Diarization", in Proc. Of ICASSP, 2007.
- [9] Aymen Chaouachi, Rashad M. Kamel, Ken Nagasaka, "Modeling and Simulation of a Photovoltaic field Based on Matlab Simulink", Conference on energy system, economy and environment, Tokyo, 2009, pp:70-74.
- [10] Gilbert M. Masters, "Renewable and Efficient Electric Power Systems". Wiley Interscience, 2004.
- [11] R.M. Kamel, A.chaouachi, K.Nagasaka, "Design and Implementation of Various Inverter Controls to Interface Distributed Generators (DGs) in Micro Grids", Conference on energy system, economy and environment, Tokyo, 2009, pp: 60-64.
- [12] R. Lasseter, K. Tomovic and P. Piagi, "Scenarios for Distributed Technology Applications with Steady State and Dynamic Models of Loads and Micro-Sources," CERTS Report, 2000.
- [13] L.I. Kuncheva, "Fuzzy Classifier Design", Physica-Verlag, Heidelberg, 2000.
- [14] O. Cordon and F.H.M.J. Jesus, A proposal on reasoning methods in fuzzy rule-based classification systems. International Journal of Approximate Reasoning. 20, 1999, pp. 21-45.
- [15] C.C. Lee, "Fuzzy logic in control systems", IEEE Transactions on Systems, Man & Cybernetics SMC-20 2, 1990, pp. 404-435.
- [16] Cornelius T.Leondes, Neural Network Systems Techniques and Applications, Volume 1 of Neural Network Systems architecture and applications, Academic Press, 1998.
- [17] E. J. Hartman, J. D. Keeler, and J. M. Kowalski, "Layered neural networks with gaussian hidden units as universal approximators," Neural Comput, 2:210-215, 1990.
- [18] Simon Haykin, Neural Networks. A Comprehensive Foundation, 2nd Edition, Prentice Hall, 1999.
- [19] Aymen Chaouachi, Rashad M. Kamel, Ken Nagasaka, "Neural Network Ensemble-Based Solar Power Generation Short-Term Forecasting", Journal of Advanced Computational Intelligence and Intelligent Informatics, Vol.14 No.1 Jan. 2010 pp. 69-75
- [20] Elisa Ricci, Renzo Perfetti, "Improved pruning strategy for radial basis function networks with dynamic decay adjustment", Neurocomputing, pp: 1728-1732, 2006.

**Aymen Chaouachi (1981)** was born in Tunis, Tunisia. He received the B.Sc. and M.Sc. degrees in Electrical Engineering from the High School of Sciences and Technologies of Tunis, Tunisia in 2004 and 2006 respectively. Since 2003, he has been with the National Institute of Research and Technology, Tunisia as researcher. Actually he is Ph.D. student in Tokyo University of Agriculture and Technology, Japan since 2008. His PhD thesis focuses on the Intelligent Management of Micro Grid.

**Rashad M. Kamel (1978)** was born in Sohag, Egypt. He received the B.Sc. and M.Sc. degrees in Electrical Engineering from Assuit University, Egypt in 2000 and 2005, respectively. Since 2001, he has been with the Electrical Engineering department, Faculty of Engineering, University of Assuit, Egypt. He started his Ph.D. in Tokyo University of Agriculture and Technology, Japan in 2007 supported by an Egyptian government scholarship. His Ph.D thesis focuses on the dynamic behavior of the Micro Grid.

**Ken Nagasaka (1956)** was born in Kermanshah, Iran. He obtained his B.S, M.S and PhD degrees in Electrical Engineering from Nihon University (1985) and Tokyo Metropolitan University (1987, 1990), Tokyo, Japan. Currently, he is an Associate Professor of Graduate School of Engineering at Tokyo University of Agriculture and Technology. Prof. Nagasaka has published more than 450 scientific papers and some of his papers won Paper-Prize such as: the Institute of Electrical Installation Engineers of Japan in 1991, three awards from the PSC in 2001, 2002 and 2006. Also in 2006, he received the Medal of the University of Tehran for his contribution to the First Conference of Control and Management of Energy Systems. His current research projects concern environmental energy engineering particularly power system analysis, power deregulation, wind power, micro-grid, load forecasting, and application of intelligent systems to power systems. Prof. Nagasaka is a member of IEE, IEIE of Japan and a member of IEEE, International Neural Network Society of U.S.A.